Research Square

Preprints are preliminary reports that have not undergone peer review.
They should not be considered conclusive, used to inform clinical practice,
or referenced by the media as validated information.

Production of PCL-Based Bilayered Nanofibrous Patches Functionalized with Human Amniotic Membrane

Huseyin Berkay Ozarici
Marmara University
Zehra Kanli
Istanbul Arel University
Mohammed Bella Jagitay
Marmara University
Semra Akkaya Turhan
Acıbadem Mehmet Ali Aydınlar University
Gamze Ozkan
Marmara University
Ayse Ceren Calıkoğlu Koyuncu
Marmara University
Canan Dogan
canan.dogan@marmara.edu.tr

Marmara University
Oguzhan Gunduz
Marmara University

Article

Keywords: Amniotic membrane, electrospinning, ocular surface diseases, PCL, Tissue Engineering, nanofiber patches

Posted Date: July 8th, 2026

DOI: https://doi.org/10.21203/rs.3.rs-10054714/v1

License: This work is licensed under a Creative Commons Attribution 4.0 International License.
Read Full License

Additional Declarations: No competing interests reported.

PRODUCTION OF PCL-BASED BILAYERED NANOFIBROUS PATCHES FUNCTIONALIZED WITH HUMAN AMNIOTIC MEMBRANE

Huseyin Berkay Ozarici[1], Zehra Kanli[1], Mohamed Bella Jagitay[4], Semra Akkaya Turhan[3], Gamze Ozkan[2], Ayse Ceren Calikoglu Koyuncu[1], Canan Dogan[1*], Oguzhan Gunduz[1]

*canan.dogan@marmara.edu.tr;

Abstract

The human amniotic membrane (AM) is a bioactive scaffold rich in collagen and extracellular matrix (ECM) proteins that promote wound healing; however, AMs direct clinical application is limited by mechanical fragility and handling challenges. Here, bilayer nanofibrous patches were fabricated by electrospinning of polycaprolactone (PCL) with AM solutions at concentrations of 3%, 5%, 7%, and 10% (w/v). Structural, physicochemical, and mechanical properties were characterized by SEM, FTIR spectroscopy, TGA, water contact angle, swelling ratio, and in vitro degradation assays. Biocompatibility and wound healing potential of the nanofibrous patches were assessed via MTT and scratch assays using human dermal fibroblasts (HDFs) respectively. Among all formulations, 7% AM-loaded patches yielded the highest cell viability while significantly accelerating wound closure ($p < 0.001$). A critical structural transition was identified at 5% AM, where fiber diameter reached its minimum, swelling ratio its maximum, and elongation at break its peak — indicating concentration-dependent disruption of the PCL matrix. These findings establish 7% AM-PCL bilayer nanofibers as a mechanically viable and biologically active platform for advanced wound care.

Keywords: Amniotic membrane; electrospinning; ocular surface diseases; PCL; Tissue Engineering; nanofiber patches

1. INTRODUCTION

Recent advancements in biomaterials and tissue engineering applications have enabled the development of functionalized systems for the treatment of several physical disorders and medical issues, providing more wellness and longevity for patients. These approaches involve the investigation of the treatment and healing processes of damaged tissues affected by various factors. To facilitate tissue repair and regeneration, drug-loaded delivery systems have been developed with potential applications in both soft and hard tissue engineering. Tissue engineering vital for disorders in the complex ocular surface region, which consists of the tear gland, eyelid, cornea and conjunctiva tissues of the eye organ, and this is compact of soft tissue.[1] Ocular surface diseases (OSDs) not only lead to serious vision loss, but also significantly reduce the quality of life of patients by causing cosmetic defects and chronic irritations. When the vital structure and complexity of the eye organ are considered, it is significant to take care of such disorders with proper treatments without damaging the tissue. OSDs occur in a wide spectrum, ranging from dry eye syndrome to severe chemical burns, infections (keratitis) and neurotrophic problems. The common consequence of these diseases is the disruption of ocular surface integrity and physiological stability.[2] Traditional approaches to treatment are generally focused on symptom management, involving the use of artificial tears, and several anti-inflammatory agents. In cases of advanced deterioration and damage, surgical procedures are applied for stabilization of the surface and tissue repair.

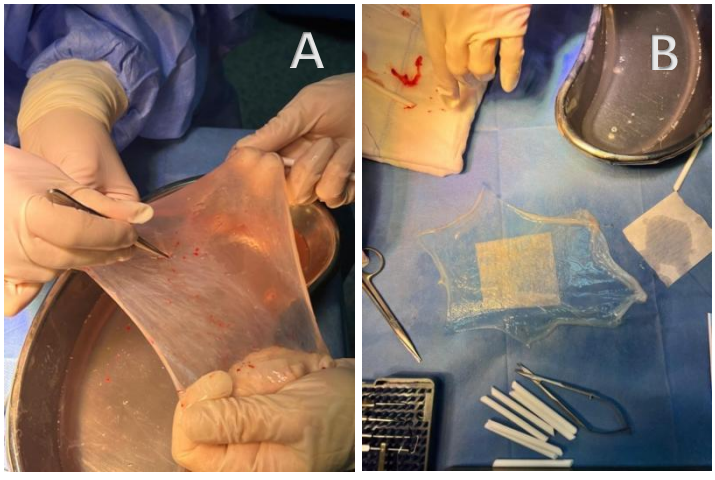


Figure 1. The cleaning procedure of AM after C-Section surgery under sterile condition. A) Before cleaning, B) After cleaning.

Traditional treatment methods generally provide temporary healing or they are insufficient in supporting full regeneration of the damaged tissue to be healed completely by itself. Especially in severe lesions that carry the risk of permanent vision loss, a biological matrix resembling the natural structure of the ocular surface, promoting stem cell migration, and providing a healing environment is necessary.[3] The lack of such an environment has boosted the interests in advanced biomaterials in regenerative medicine. Tissue engineering principles highlighted the use of several biomaterials to overcome the limitations in traditional treatment methods. Biomaterials allow the development of micro/nanostructures that support cell adhesion and proliferation, serving as a temporary scaffold for damaged tissue to repair ocular surface damage.[4] Synthetic biopolymers, especially polycaprolactone (PCL), have been widely researched in this field due to their controlled degradation rates and excellent biocompatibility. It is also an FDA-approved, hydrophobic, and biocompatible material.[5] Yet, synthetic polymers could be insufficient in terms of providing bioactivity.

At this point, the superior regenerative properties of natural biomaterials, especially AM, are noteworthy.[6] As seen in Figure 1, AM derived from human placenta has long been considered the gold standard for ocular surface reconstruction because it has a strong extracellular matrix (ECM) rich in anti-inflammatory, anti-angiogenic and wound-healing molecules such as collagens, hyaluronic acid, proteoglycans, fibronectins, growth factors , and other bioactive components.[7] Despite these superior properties of the AM, its limited mechanical integrity and durability necessitate more stable and specialized carrier systems. The known superior wound healing, anti-inflammatory, and anti-angiogenic properties of the AM make it valuable as a biomaterial for ocular surface reconstruction. However, as a natural biomaterial derived from living tissue, the use of AM alone has limitations in terms of mechanical durability and degradation rate. The valuable ECM components contained in AM, such as Type IV, V, and VII collagens, epidermal growth factor (EGF), fibroblast growth factor (FGF), transforming growth factor-ß (TGF-ß), and specialized proteins provide an ideal environment for cellular regeneration, creating the need to combine this bioactivity with a durable structural scaffold. In this study, the regenerative components of AM were integrated with PCL as it has high mechanical strength and slow degradation rate.[6,8,9] Electrospinning offers the production of a controlled micro-nanofiber architecture and low-cost fabrication.[10] The key innovation of this study is the development of a bilayer patch that combines two distinct functions within a single structure to support multifaceted

ocular surface healing. Significantly, this work distinguishes itself from the literature by incorporating two different nanofibrous layers: one containing collagen, hyaluronic acid and PRP, and the other one as amniotic membrane. The PRP-containing layer also plays a role as a protective layer with patient-specific properties. To the best of our knowledge, AM nanofibers incorporated with PRP have not yet been investigated in the literature.

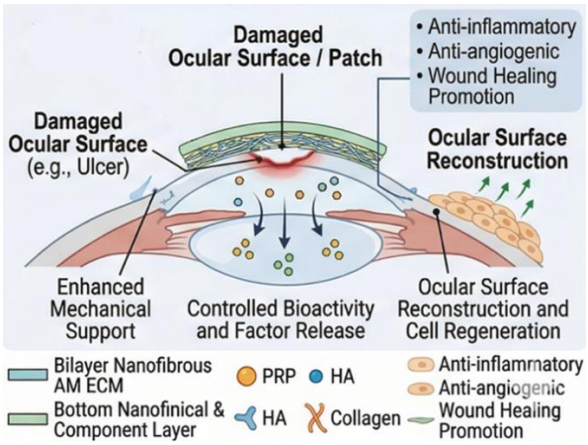


Figure 2. Application of produced fibers from obtaining of AM on the tissue.

This study aims to evaluate the effects of 4 bilayer patches produced with 4 different concentrations of AM, as shown in Figure 2. The first layer encapsulates the dissolved AM ECM encapsulated by PCL to provide regenerative components, while the second layer contains PCL along with additional supporting biocomponents: PRP, HA, and Collagen. This bilayered, PRP-infused nanofibrous architecture aims to optimize mechanical strength by providing long-term structural support and accelerate the wound healing process by creating a biologically active site that mimics the native ECM with regenerative factors. The fiber morphology and diameter distribution were confirmed by SEM analysis. The integration of AM into the PCL-based matrix, enriched with PRP, HA, and Collagen, was designed to modulate the surface wettability and thermal stability of the scaffolds. Furthermore, the interplay between the hydrophobic PCL backbone and the hydrophilic AM content is expected to regulate the swelling behavior and degradation kinetics, thereby maintaining structural integrity during the healing period. It is hypothesized that tuning these physicochemical properties creates a biocompatible microenvironment that not only supports cell viability (MTT assay) but also enhances cell migration (scratch assay), ultimately accelerating the wound healing process through a synergistic combination of structural support and biological signaling.

2. Results & Discussion

SEM of Nanofibers

The morphology and diameter distribution of the electrospun nanofibers were systematically evaluated via SEM analysis. Theoretically, an increase in AM concentration is expected to enhance the electrical conductivity of the spinning solution due to the inherent ionic nature of the biological proteins and salts within the AM and both of the layers are integrated successfully (Figure 3). This increased conductivity typically promotes greater jet stretching under the electric field, thereby resulting in finer fiber diameters. Consistently, a reduction in fiber diameter was observed for the 3% AM concentration and 5% AM concentration groups (Figure 4a, 4b). However, a deviation from this linear trend occurred at higher concentrations; the fiber diameters in the 7% AM concentration group exhibited a slight increase relative to the 5% AM concentration group (Figure 4c). This phenomenon became more pronounced in the %10 AM concentration group. While the higher AM content (10%) was anticipated to produce the thinnest fibers due to maximum conductivity, the results suggest that solution viscosity became the dominant parameter at this stage (Figure 4d). The increased viscosity of the AM solution likely hindered the extensive stretching of the polymeric jet during the electrospinning process, ultimately leading to the formation of fibers with larger diameters.[11] These observations indicate a complex interplay between conductivity and viscosity, where a critical concentration threshold dictates the transition of the primary factor governing fiber attenuation.[11,12]

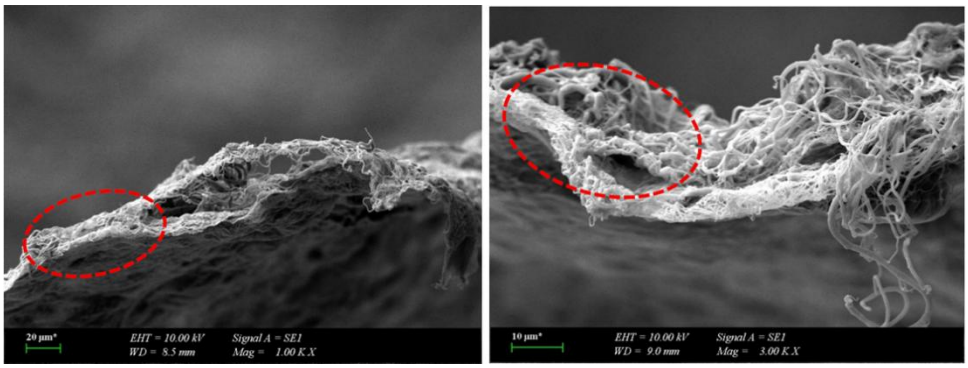


Figure 3. SEM image of cross-sectioned bilayer fiber patch.

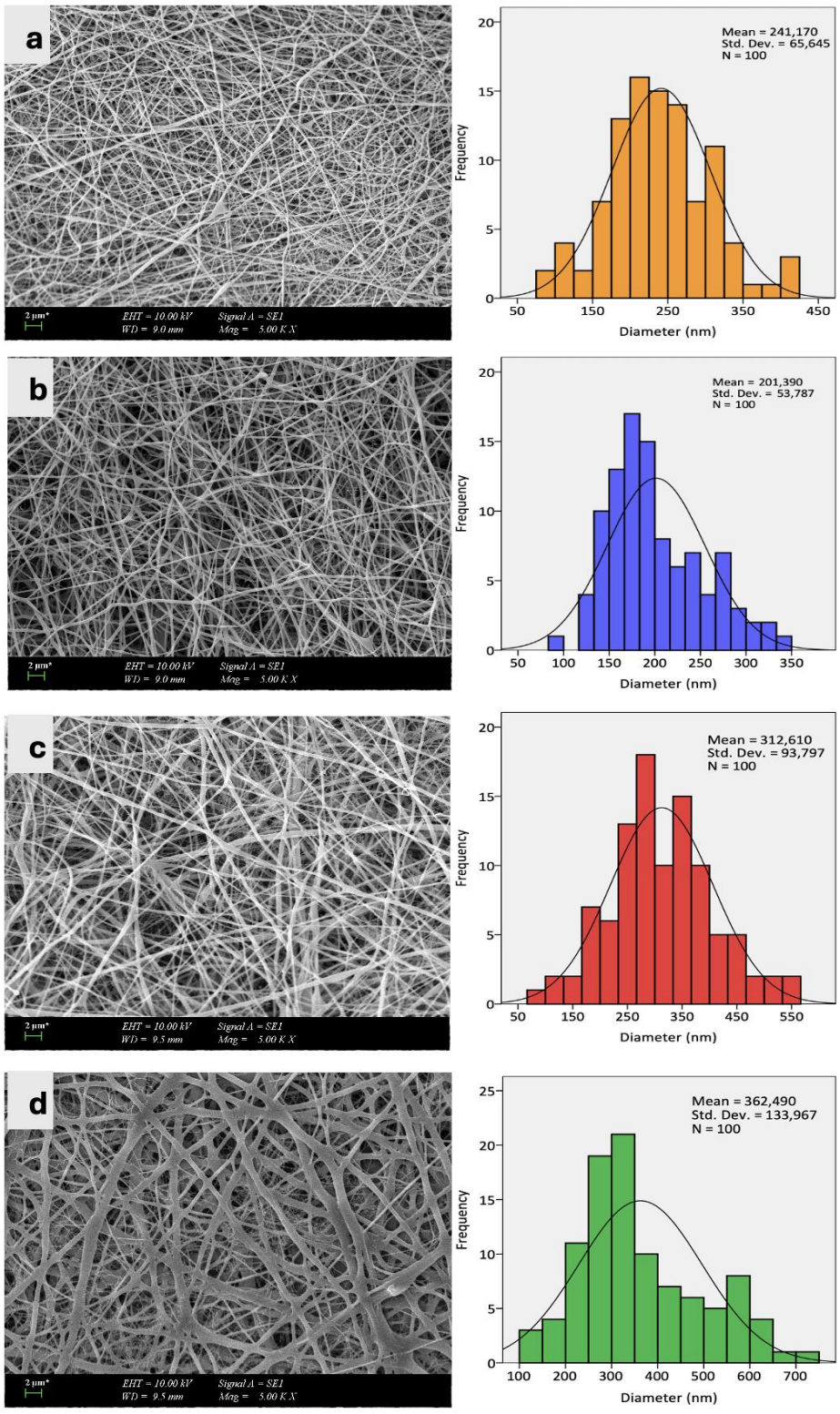


Figure 4. The bilayer fibers with their diameter measurements, which a) 3% AM concentration, b) 5% AM concentration, c) 7% AM concentration and d) 10% AM concentration.

FTIR Spectroscopy for the Evaluation of Chemical Structure of Nanofibers

FTIR spectroscopic analysis of the processed amniotic membrane (AM) clearly identified characteristic absorption bands corresponding to the essential ECM components, including collagenous proteins, glycosaminoglycans, and lipids. In the high-wavenumber region, a broad absorption band observed between 3270 and 3300 cm^{-1} was assigned to the Amide A band, originating from the N-H stretching vibrations of peptide bonds and overlapping hydroxyl (O-H) group vibrations within the proteinaceous matrix (Figure 5a1).

The most prominent feature of the spectrum, the Amide I band, was recorded within the 1630 – 1650 cm^{-1} range, as shown in Figure 6c and 6d, representing the carbonyl (C=O) stretching vibrations of the collagen backbone.[13] The intensity and well-defined profile of this peak serve as a critical indicator for the preservation of the collagenous triple-helix architecture following the stabilization processes.[14] Furthermore, the absorption peaks identified in the 1000 – 1100 cm^{-1} region, associated with C-O stretching vibrations, confirm the presence of hyaluronic acid and various glycosaminoglycans (GAGs) inherently abundant in the AM structure (as shown in Figure 5a2). These findings collectively validate that the bioactive composition of the amniotic membrane was successfully maintained throughout the scaffold fabrication stages. [15,16]

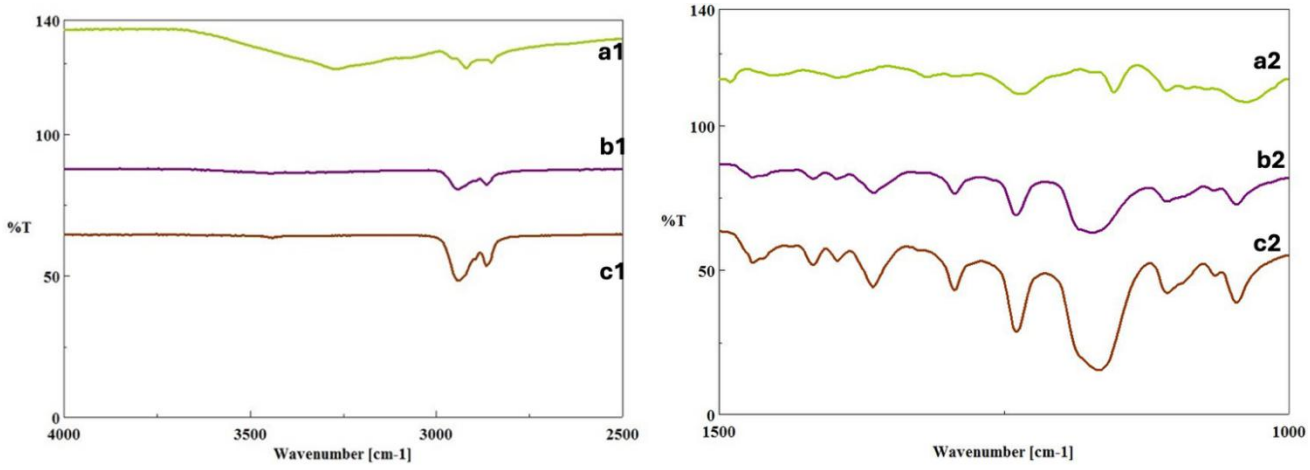


Figure 5. The peaks of a1) AM, b1) PRP-COL-HA-PCL layer, c1)PCL are shown in the 2500-4000 cm^{-1} region, and a2)AM, b2) PRP-COL-HA-PCL layer and c2) PCL are shown in 1000-1500 cm^{-1}.

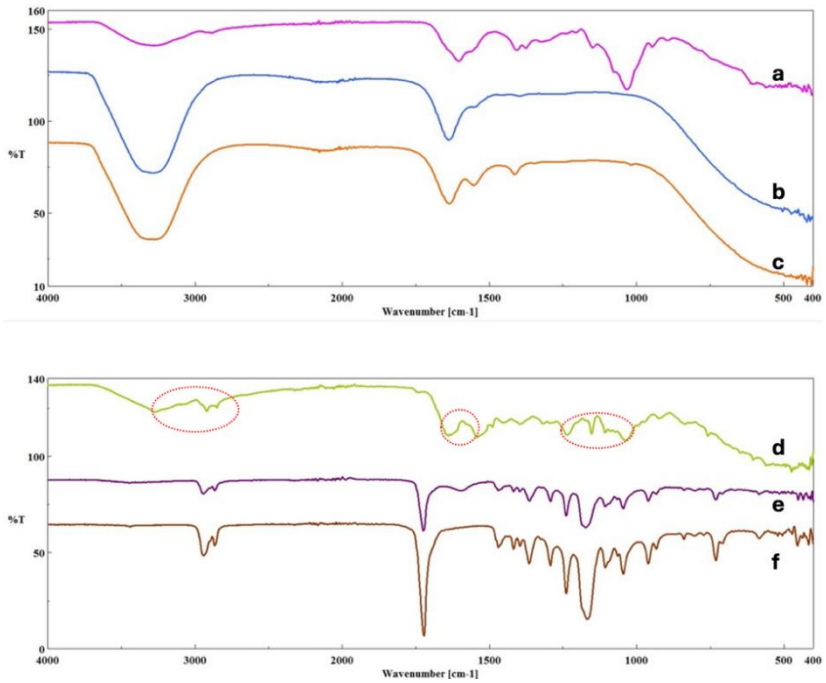


Figure 6. Overlay FTIR spectra of a) Hyaluronic acid (HA), b) PRP, c) Collagen (COL), d) Amniotic membrane (AM), e) PCL-PRP-COL-HA layer, and f) PCL.

The chemical composition of the composite nanofibers—comprising polycaprolactone (PCL) as the encapsulating matrix for collagen (COL), platelet-rich plasma (PRP), and hyaluronic acid (HA)—was evaluated through comparative FTIR spectroscopy (Figure 6a, 6b, 6c). The overlay of spectra from the pure components and the final composite structure confirmed the successful integration of these bioactive agents (Figure 6e).

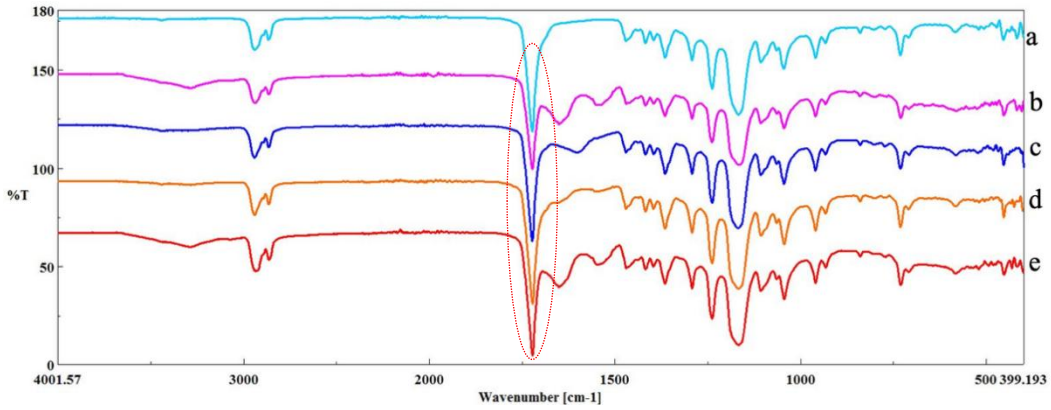


Figure 7. The spectra of the bilayer AM patches with a) PCL, b) 10% concentration, c) 5% concentration, d) 3% concentration, e) 7% concentration.

The most dominant and sharpest feature in the composite spectrum was the characteristic band at around 1720 cm^{-1}, assigned to the carbonyl (C=O) stretching vibrations of the ester groups within the PCL backbone (Figure 7a). The high intensity and well-defined sharpness of this peak validate that PCL maintained its structural integrity and functioned effectively as the primary supporting scaffold for the biological additives. Furthermore, the absence of significant shifts in this characteristic PCL peak suggests that the incorporation of COL, PRP, and HA occurred primarily through physical entrapment and intermolecular interactions within the nanofibrous matrix rather than altering the fundamental chemical structure of the polymer.

Mechanical Testing of Nanofibers

The mechanical performance of the electrospun nanofibers was evaluated based on the tensile strength and elongation at break (%) values summarized in Table 1.

Table 1. Mechanical strength values of the fibers.

Materials	Tensile Strength (MPa)	Elongation at Break (%)
PCL	11,96±3,23	24,85±3,05
AM	1,82±0,45	37,80±3,16
PCL-PRP-COL-HA	2,096±1,33	26,63±3,13
3% Bilayer	9,08±1,78	14,02±4,66
5% Bilayer	6,65±0,65	29,5±6,04
7% Bilayer	3,92±0,75	21,71±1,62
10% Bilayer	3,31±0,68	9,54±1,06

The pure PCL control group exhibited the highest tensile strength (11.96 ± 3.23 MPa), which can be attributed to the continuous and well-aligned chain structure of the synthetic polymer matrix, as can be seen in Table 1. Upon the fabrication of bilayer patches, a concentration-dependent decrease in tensile strength was observed: 9.08 MPa, 6.65 MPa, 3.92 MPa, and 3.31MPa for the 3%, 5%, 7%, and 10% bilayer groups, respectively. This inverse correlation suggests that the incorporation of the amniotic membrane (AM) introduces structural discontinuities and acts as a stress-concentrator within the semi-crystalline PCL matrix. [16] Beside polymers and patches, AM

exhibited the lowest tensile strength yet, showed the highest elongation break (1,82±0,45 MPa and 37,80±3,16 %) as shown in Table 1. The tensile test applied on AM is shown in Figure 8.

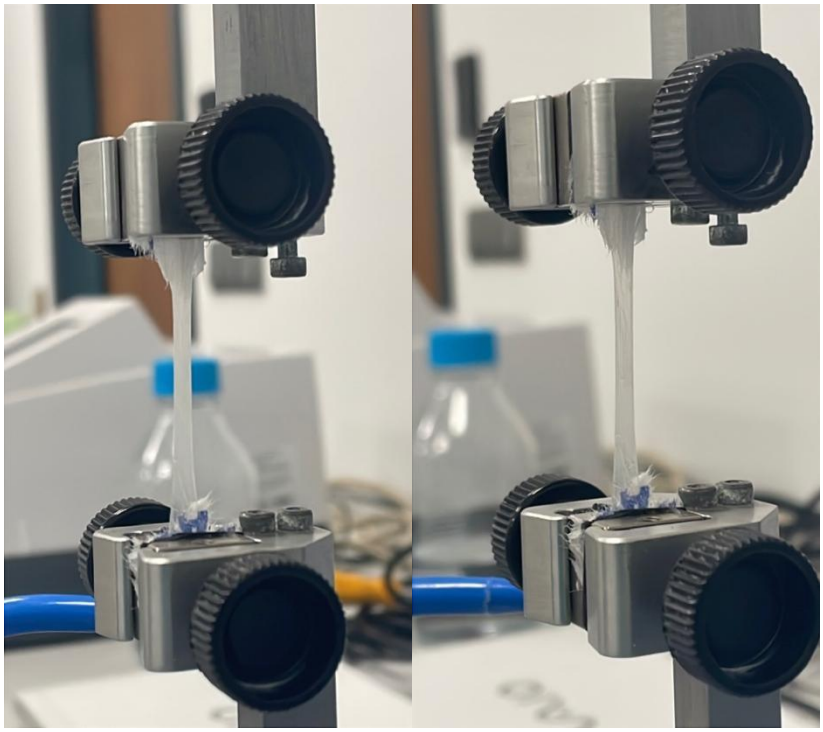


Figure 8. Tensile strength test applied on AM

Although AM showed the lowest tensile strength among the groups, it exhibited the highest elongation break percentage (37,8%). This can be attributed to the irregular wavy structural architecture of the biological material. AM has several interconnected and intertwined collagens embedded within proteoglycans, then becomes unravel and stretch when a load is applied. On the other hand, PCL has higher tensile strength than AM does. Due to its flexible polymer chain structure, PCL exhibits superior elasticity and elongation capacity compared to AM, which is relatively less elastic and therefore more susceptible to mechanical deformation.[17].[18]

Interestingly, the elongation at break values exhibited a non-linear trend. The pure PCL group showed an elongation of 24.85%, while the 5% AM concentration group reached the maximum flexibility among all nanofiber groups (29.5 ± 6.04 %). This enhancement in ductility at a 5% AM concentration resulted in the formation of thin fibers. Thus, these thinnest fibers with high surface to volume ratio caused higher elongation at break.[19] However, a dramatic reduction in elongation

was noted as the AM concentration reached 10% (9.54%). This shift towards brittle behavior is likely due to the excessive aggregation of AM particles at high concentrations, which physically hinders the sliding of polymer chains and leads to premature mechanical failure.[16]

TGA Analysis of Nanofibers

Thermogravimetric analysis (TGA) and derivative thermogravimetry (DTG) were employed to evaluate the thermal stability, decomposition temperatures, and relative weight percentages of the bilayer nanofibrous constituents. The TGA and DTG profiles for the 3%, 5%, 7%, and 10% bilayer fibers are shown in Figure 9, with the temperature range extending from ambient conditions to 600°C.

The primary TGA curves (left Y-axis) depict the progressive mass loss as a function of temperature, initiating from the 100% baseline. This non-continuous degradation typically corresponds to the successive evaporation of residual moisture and the subsequent thermal combustion of the biological and polymeric components.[19] Concurrently, the DTG curves (right Y-axis, indicated by the green profiles) represent the rate of weight loss (%/°C). These derivative peaks allow for the precise identification of the maximum degradation temperatures (T_{max}) for each component within the composite structure, providing insights into the thermal interactions between the PCL matrix and the incorporated biocomponents.[20]

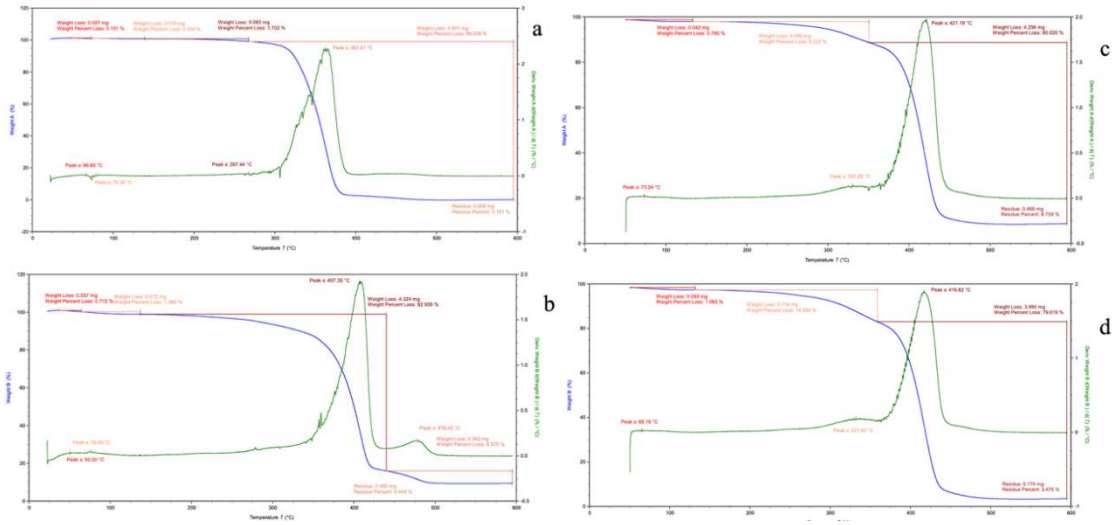


Figure 9. TGA analyze results. DTG graphs of a) 3% AM-PCL bilayer b) 5% AM-PCL bilayer, c) 7% AM-PCL bilayer and d) 10% AM-PCL bilayer.

The thermal degradation profiles of the bilayer scaffolds provided substantial evidence of their composite nature. Before the primary pyrolysis phase of the PCL matrix (typically occurring between 300°C and 400°C), distinct secondary peaks or 'shoulders' were detected. These features are attributed to the early thermal decomposition of the hydrophilic biocomponents, specifically PRP, HA, and collagen.[21] In the 3% AM concentration group, a premature degradation peak was identified at 267.44°C (Figure 9a), suggesting that at lower concentrations, the biological phase may be insufficiently encapsulated, or in other words, 'protected' by the polymer matrix, leading to accelerated thermal breakdown.

In contrast, the 7% AM concentration and 10% AM concentration groups exhibited a more stable degradation shoulder within the 330°C–331°C range (Figures 9c and 9d). This pyrolytic region corresponds to the controlled thermal degradation of the integrated organic phase. Notably, the 10% group demonstrated a higher mass loss (14.28%) in this specific phase, validating the successful incorporation of a higher biological load. The shift in degradation temperatures indicates that increasing the biological concentration from 3% to 7% enhances the thermal resistance of the composite by approximately 60°C. This significant improvement is likely due to the formation of a denser, interconnected biological polymer network that acts as a thermal barrier, delaying heat transfer and stabilizing the overall structure.[22]

Contact Angle Measurement of Nanofibers

Surface wettability is a crucial parameter for maintaining initial cell adhesion, spreading, and subsequent proliferation on biomaterial scaffolds.[23] In this study, the hydrophilic character of the electrospun bilayer patches was quantitatively evaluated through static water contact angle (WCA) measurements (Table 2). The incorporation of bioactive components—specifically (HA), (PRP), and (AM)—significantly modulated the surface energy of the PCL matrix. While pure PCL is inherently hydrophobic with a high contact angle, the presence of these hydrophilic agents, which are rich in hydroxyl and amine functional groups, facilitated a transition toward a more wettable surface.[24] This increased hydrophilicity is expected to enhance the interaction between the scaffold

and the aqueous biological environment, thereby promoting a favorable microenvironment for the attachment of human dermal fibroblasts (HDFs) on nanofibers.

Table 2. Contact Angles of the Produced Fibers.

Samples	Contact Angles (º)
PCL	113.93
3% Bilayer	107.47
5% Bilayer	118.46
7% Bilayer	103.32
10% Bilayer	87.44

As anticipated, the incorporation of bio-additives led to a concentration-dependent decrease in WCA) values. Specifically, the WCA decreased from 113.93° for pure PCL to 107.47°, 103.32°, and 87.44° in the nanofibers containing 3%, 7%, and 10% AM, respectively. (shown in Figure 10). A notable exception was observed in the 5% AM concentration group. This deviation can be explained by the synergistic effect of its unique morphological and mechanical properties. As aforementioned, the 5% AM concentration group exhibited the thinnest fiber diameter and the highest elongation at break (29.5%) (Table 1). From a surface physics perspective, a reduction in fiber diameter significantly enhances the specific surface area of the material. These finer nanofibers provide a considerably higher surface-to-volume ratio, thereby maximizing the available contact points for water molecules to interact with the polymer matrix. This feature also decreased the porosity of the nanofibrous structure. These findings suggest that the wettability of these scaffolds is governed not only by their chemical composition but also by the intricate architecture of the nanofibrous network.[25]

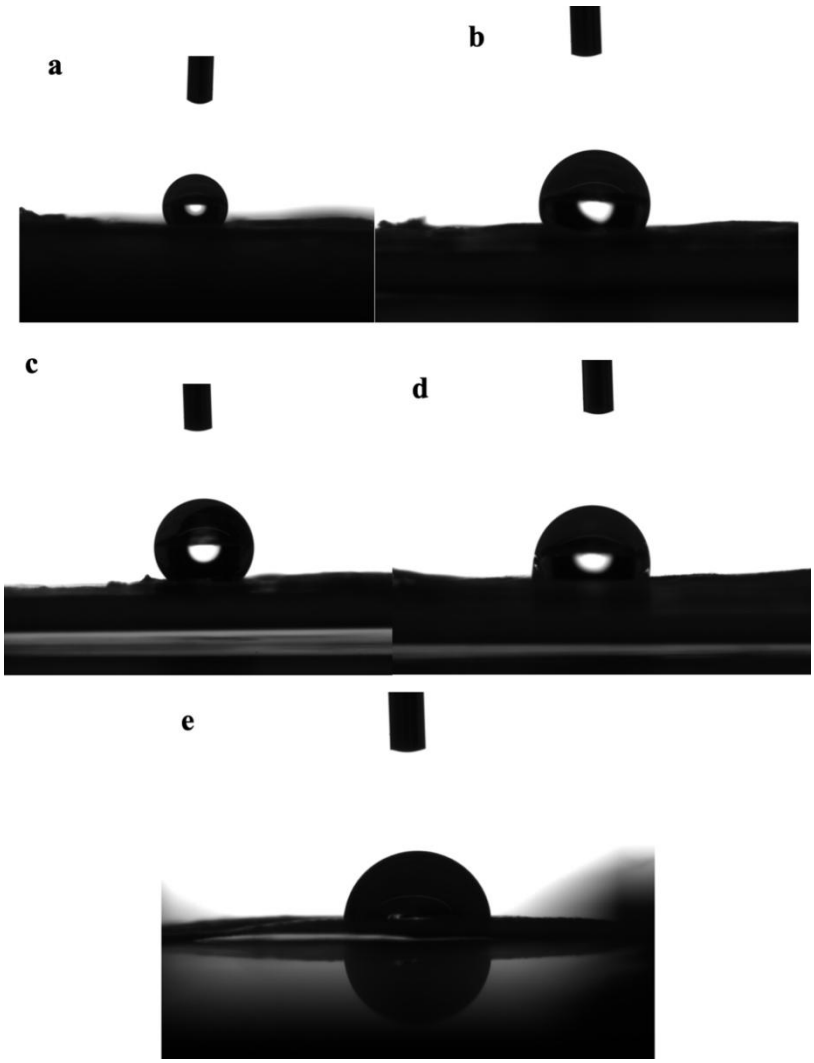


Figure Error! No text of specified style in document.**10.** Contact Angle of the fibers of a) PCL fiber, b) 3% AM concentration fiber, c) 5% AM concentration fiber, d) 7% AM concentration fiber and e) 10% AM concentration fiber.

Swelling Behaviour of Nanofibers

The swelling behavior of the electrospun bilayer patches provides essential insights into their liquid absorption capacity and structural stability under physiological conditions. The water-holding capacities of the scaffolds (3%, 5%, 7%, and 10 % w/v AM) were monitored in PBS (pH 7.4) over a 14-day period. The hydrophilic nature of the (AM) initially facilitated water penetration across all groups. The highest swelling ratio was recorded in the 5% AM group, Interestingly, further increasing the AM concentration to 7% and 10% resulted in a stabilization

and even a relative decrease of the water-holding capacity, with values at day 14, mirroring those of the 3% group (Figure 11.)

This non-linear trend suggests that the 5% AM concentration represents a critical structural threshold within the PCL matrix. The superior swelling capacity of the 5% AM group can be attributed to its unique morphology: the lower fiber diameter identified in this group significantly increases the specific surface area and porosity, allowing for enhanced capillary action and water entrapment. Conversely, at higher concentrations (7% and 10%% w/v), the increased biological component load and potential fiber aggregation may restrict the available pore volume, thereby limiting the maximum swelling capacity.[26, 27]

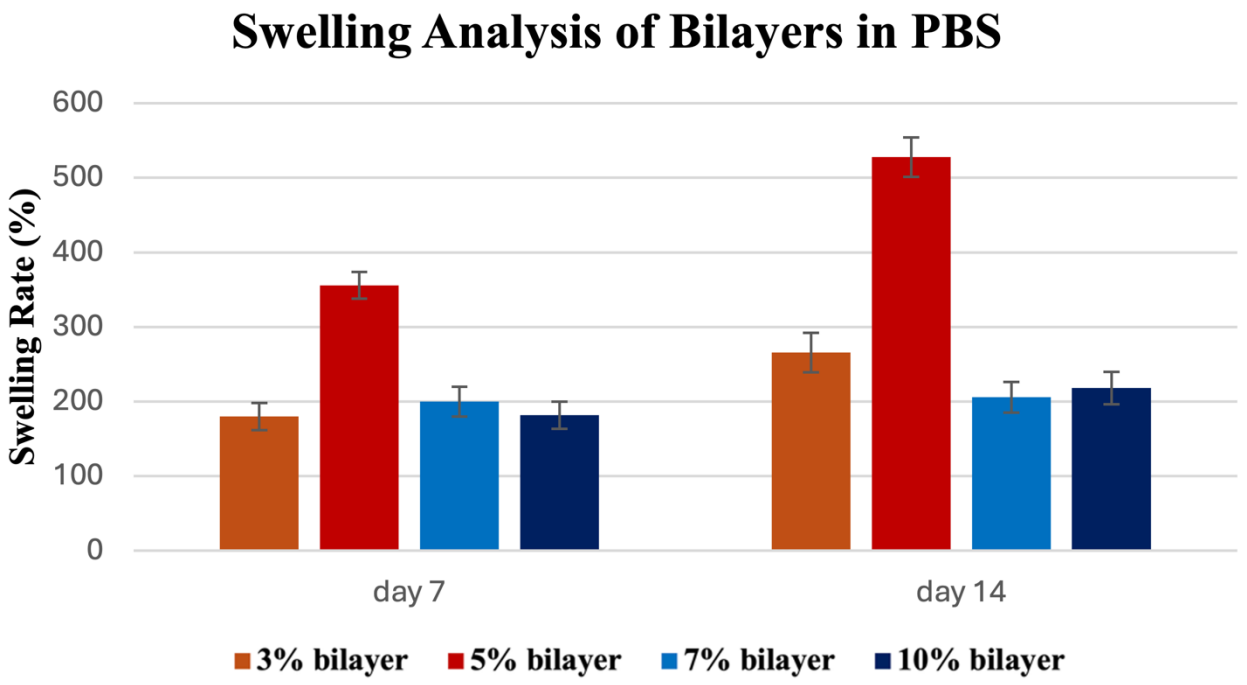


Figure 11. The swelling chart of the fibers by rate (%).

Degradation Behaviour of Nanofibers

The biodegradability of the electrospun bilayer patches was monitored over a 14-day period by measuring the mass loss in PBS medium as shown in Figure 12. As anticipated, all experimental groups exhibited a progressive weight loss; however, the degradation kinetics were significantly influenced by the (AM) concentration. The 3% group demonstrated the highest structural stability, retaining approximately 90% of its initial mass by day 14 (10% degradation rate).

Conversely, increasing the AM content generally accelerated the degradation process. The 10% AM group exhibited the highest weight loss, reaching 14% by day 7 and 26% w/v by day 14. This accelerated degradation is attributed to the high density of hydrophilic natural proteins and bioactive components, which facilitate faster dissolution and release into the aqueous environment.

A critical finding was the unique degradation profile of the 5% AM group. While its mass loss was comparable to the 3% AM and 7% AM groups during the first week (~7–8%), it experienced a dramatic acceleration between days 7 and 14, ultimately reaching a degradation level of 23%. This observation directly correlates with the swelling behavior discussed in the previous section. The superior water-holding capacity of the 5% AM group allows water molecules to penetrate deeper into the fibrous matrix, thus facilitating more extensive hydrolytic degradation of the polymer chains. These results confirm that the 5% AM concentration inherently optimizes both water uptake and subsequent biodegradability, which are essential for synchronized tissue regeneration and scaffold resorption.

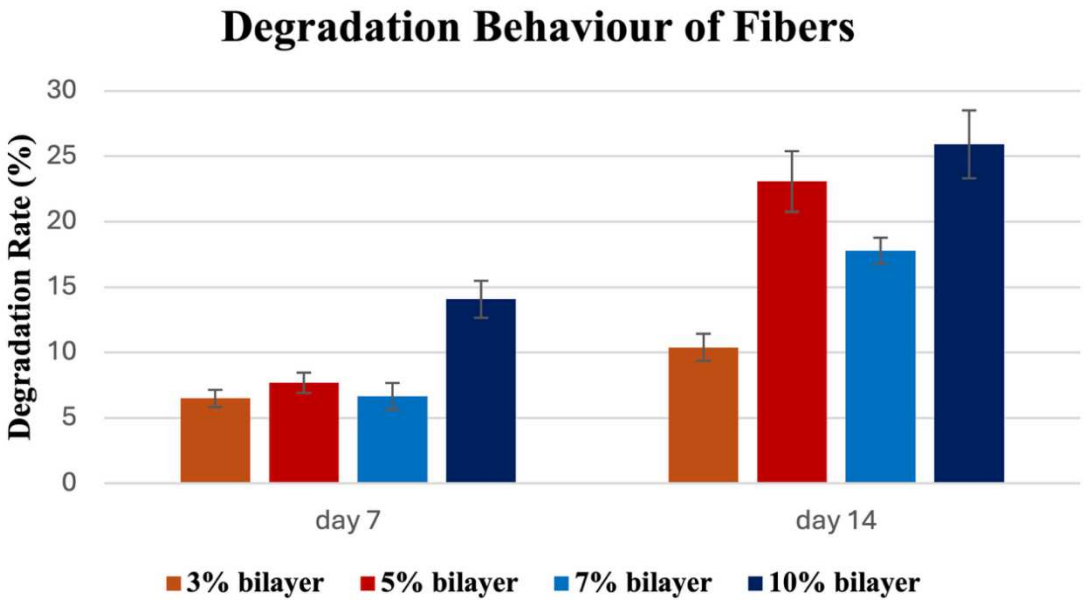


Figure 12. The diagram showing degradation rate (%) of the fibers.

MTT Assay of Nanofibers

The cytocompatibility of the electrospun bilayer patches and the influence of (AM) concentration on cellular behavior were evaluated via the MTT assay using (HDFs). The percentage of cell viability was monitored over a 7-day period, providing a comparative analysis of the different fiber groups on days 1, 3, and 7.

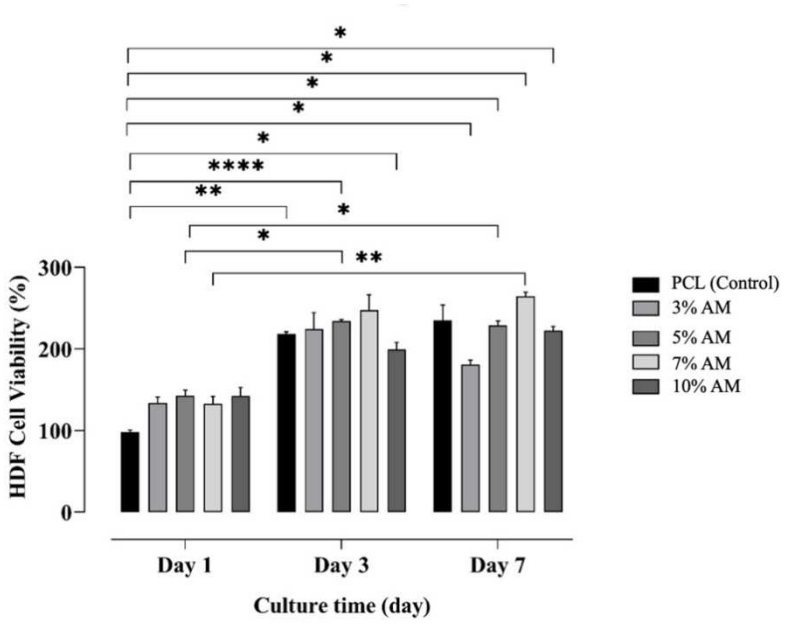


Figure 13. Biocompatibility of AM concentration groups in HDF cells was evaluated by the MTT assay. Cell viability was measured on days 1, 3, and 7 and expressed as percentage (%) relative to the PCL (control) group. Data are presented as mean ± SEM (n = 3). Statistical analysis was performed by two-way ANOVA followed by Tukey's multiple comparisons test; significance levels are indicated as $p < 0.05$, $p < 0.01$, $**p < 0.001$, and $***p < 0.0001$.

The MTT cell viability analysis showed that the bilayer patches (3%, 5%, 7% and 10% AM) were highly cytocompatible with (HDFs), with correlation of the cellular response exhibiting a clear concentration-dependent trend, as can be observed in Figure 13. On Day 1, all (AM)-integrated groups exhibited higher cell attachment and viability than the pure PCL control group. By Day 3, a substantial increase in cell viability was observed across all experimental groups, with statistically significant differences emerging among the various AM concentrations and time points ($*p< 0.05$; $**p< 0.001$; $***p<0.0001$).

By Day 7, the highest cell viability was measured in the 7% AM group ($**p< 0.01$), indicating this concentration as the most favorable environment for HDF proliferation. In contrast, the 3% AM group showed comparatively lower viability levels than the other bilayered patches at this time point. While higher concentrations (10% AM) also supported viability, the 7% threshold appears to maximize the proliferative signal without the potential restrictive effects of excessive protein density on the nanofibrous topography. The superior performance of the 7% AM group

suggests that a 7% AM concentration provides an optimal balance between the availability of bioactive factors and a scaffold architecture that supports nutrient exchange.

Scratch Assay of Nanofibers

The influence of the bilayered nanofibers on the migration and repopulation of (HDFs) was evaluated via a scratch assay. At the initial time point (0 h), the scratch widths were standardized and comparable across all experimental groups. Following 24 h of incubation, the control group exhibited substantial wound closure; however, the migration rates in the (AM)-loaded groups varied significantly according to the AM concentration. The 7% AM group demonstrated the highest wound-healing performance among the AM-containing groups and showed a wound-closure profile comparable to the control group, indicating that a 7% AM concentration may be optimal for supporting fibroblast migration (Figure 14). In contrast, the 5% AM group maintained a more pronounced open wound gap, suggesting a slower migration rate at this specific concentration. While the 3% AM group exhibited a better closure profile than 5% AM, its performance remained lower than that of the control and 7% AM groups. The 10% AM group showed only partial closure, potentially due to the higher protein density that slightly hinders the rapid mobility of the cells. Overall, these findings, indicate that wound closure is highly sensitive to AM concentration, with the 7% AM formulation providing the most favorable microenvironment for accelerated wound healing. From quantitative analysis (shown in Figure 15), the result supports the scratch assay shown in Figure 14.

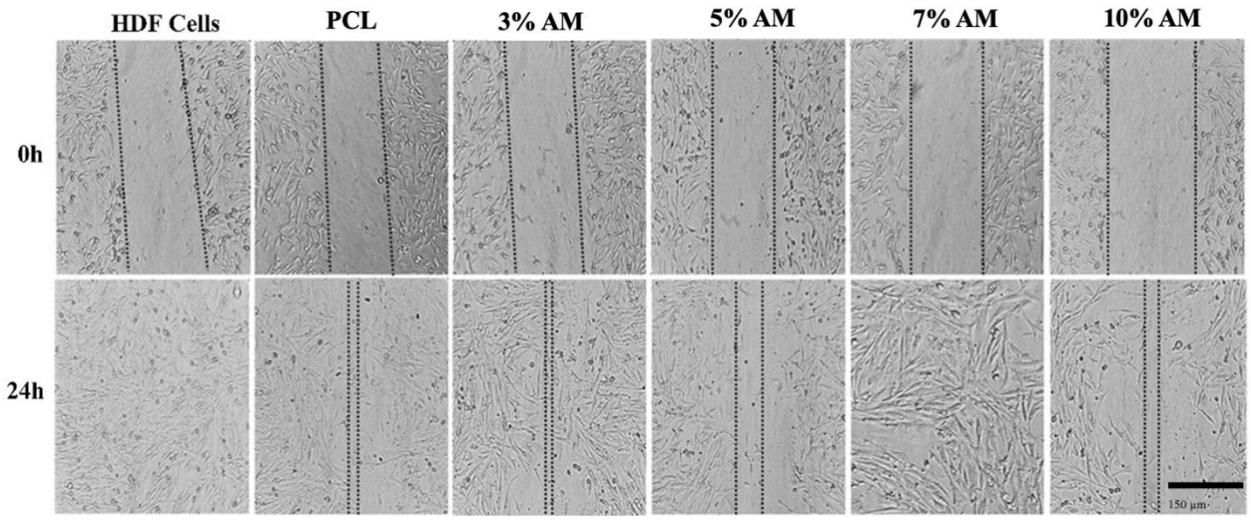


Figure 14. Scratch (wound healing) assay in HDF cells. Representative microscopic images of the scratch area at 0 h and 24 h are shown for the control (HDF cells)**,** PCL**,** 3**%,** 5**%,** 7**%,** and 10**%** AM (w/v) groups. Dashed lines indicate the wound margins (scratch edges). Images were acquired at 10× magnification **(**scale bar = 150 µm**).**

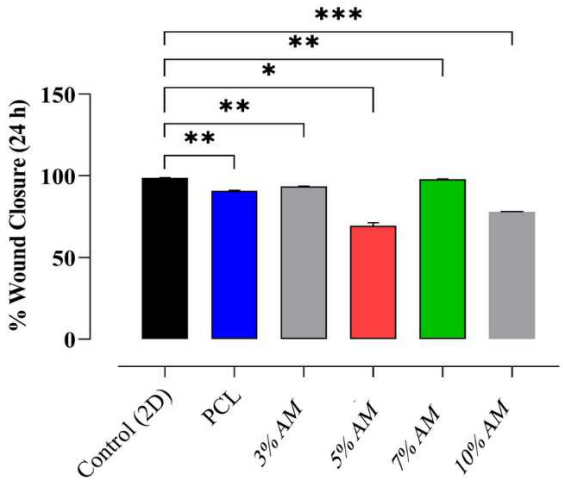


Figure 15. Quantitative analysis of the wound-healing capacity of HDF cells across different nanofiber groups, expressed as the percentage of wound closure at 24 h post-scratch regarding control group. Images were analyzed using ImageJ, and the percentage wound closure was calculated using the standard formula. Data are presented as mean ± SEM (n = 3). Statistical significance was determined by one-way ANOVA followed by Tukey's multiple comparisons test.

3. Materials & Methods

3.1. Materials

Formic acid (98-100%, Sigma Aldrich, USA) and acetic acid (glacial 100%) (Sigma Aldrich, USA) were used as solvents , Polycaprolactone (PCL) (80,000 Mw, Sigma Aldrich) was used as a carrier polymer. (AM) was obtained from Ethics Committee for Non-Pharmaceutical and Non-Medical Device Clinical Research of Marmara University, Faculty of Medicine with ethical committee's permission (protocol no:09.2025.25-0704). HA, collagen and PRP were used in the second layer of the fiber patch. PRP was obtained with ethical committee permission from Ethics Committee for Non-Pharmaceutical and Non-Medical Device Clinical Research of Marmara University, Faculty of Medicine (protocol no:09.2025.25-0704). Collagen (20 mg/ml) was purchased from Bugamed, Türkiye, and hyaluronic acid was purchased from Akcan Chemical, Türkiye. Informed consent was obtained from all subjects and/or their legal guardian(s), and all methods were performed in accordance with the relevant guidelines and regulations.

3.2. Preparation of Solutions

Preparation of Freeze-Dried Amniotic Membrane

A binary solvent system consisting of formic acid and acetic acid (v/v ratio) was employed for the dissolution of all components. Human AMs, obtained following elective Cesarean section, were initially preserved in a mixture of Dulbecco's Modified Eagle Medium (DMEM) and glycerol to maintain structural integrity during low-temperature storage. Prior to processing, the membranes were thawed, thoroughly rinsed with distilled water to eliminate residual DMEM and glycerol, and subsequently stored at -80 °C. The frozen AM samples were then subjected to lyophilization for 72 hours. Post-lyophilization, the membranes were collected and maintained at ambient temperature.

Preparation of Amniotic Membrane Solution

To facilitate dissolution and optimize the surface-to-volume ratio, the dried membranes were fragmented into small pieces. AM solutions were prepared at four concentrations (3%, 5%, 7%, and 10% w/v). Concurrently, a 20% (w/v) polycaprolactone (PCL) solution was prepared separately in 10 mL of the aforementioned solvent system and stirred at rpm at room temperature

for 3 hours. The AM solutions were similarly homogenized using a magnetic stirrer at 250 rpm and a constant temperature of 38 °C.

Solutions were mixed in a separate beaker with the ratio of 1:1. 5 ml of PCL solution and 5 ml of amniotic membrane solution were taken and mixed at 250 rpm without heat for 20 minutes (Figure 16). All different concentration solutions were prepared in the same way.

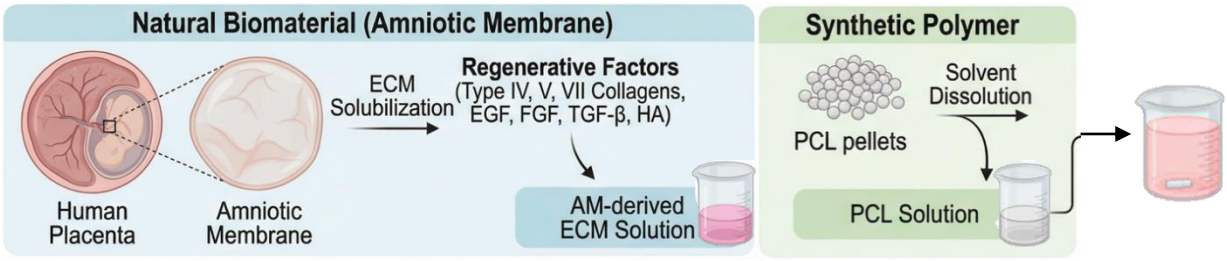


Figure 16. The mixture of dissolved AM solution and PCL solution for electrospinning.

Preparation of Collagen-PRP-Hyaluronic Acid Solution

To fabricate the bilayer patch, the secondary layer was prepared by initially dissolving 20% (w/v) PCL in the binary solvent system. Following complete dissolution (approximately 3 hours), 60 mg of hyaluronic acid was incorporated into the PCL matrix. The collagen component was prepared using two distinct methods: first, 10 mL of Type I collagen pH 7.4 (mg/mL) was transferred to a Petri dish and dehydrated in an oven at 40°C overnight; subsequently, 0.25 g of the resulting dry collagen powder was added to the PCL solution. Any remaining undissolved collagen powder was also directly integrated into the polymer blend. Concurrently, (PRP) samples were thawed from storage at -80 °C, and 1 mL of the PRP supernatant was introduced dropwise into the PCL/collagen/hyaluronic acid mixture during continuous magnetic stirring to ensure a homogeneous composite solution.

Preparation of Nanofibrous Patches via Electrospinning

The prepared solutions were loaded into 10 mL BD syringes and processed using a commercial electrospinning system (NS24, Inovenso Co., Türkiye). To facilitate the process, a polyethylene plastic tube was connected between the syringe tip and a 20G stainless steel needle. The

electrospinning parameters were maintained at a constant flow rate of 0.5 mL/h and an applied voltage of 17 kV. Each electrospinning session lasted approximately 3 hours to ensure sufficient fiber deposition. As a control group, a 20% (w/v) PCL solution without biological components was electrospun under identical conditions (Figure 17).

Five experimental groups were established: a pure PCL fiber group (Control) and four bilayer groups containing varying concentrations of (AM) in the primary layer, corresponding to final AM contents of 3%, 5%, 7%, and 10%.

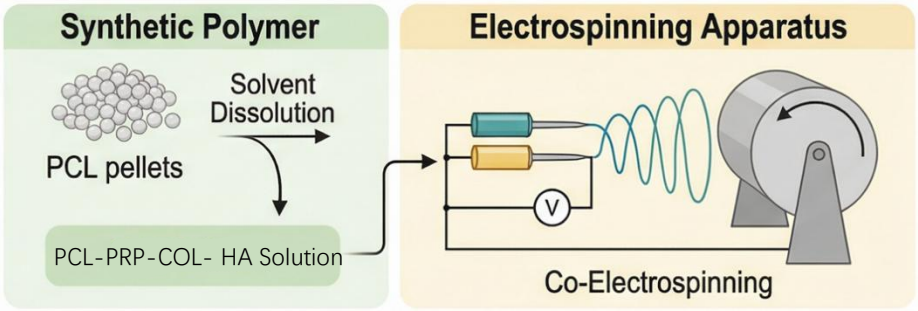


Figure 17. Production of the second layer

3.3. Characterization of Nanofibers

Scanning Electron Microscopy ***SEM***

The morphological characteristics of the fabricated bilayer fibers, containing varying concentrations of amniotic membrane, were examined via SEM (EVO LS 10, ZEISS). Prior to imaging, the samples were sectioned into small fragments and mounted on stubs. To ensure adequate surface conductivity and minimize charging effects, the specimens were sputter-coated with a gold-palladium (Au-Pd) alloy for 120 seconds using a Quorum SC762 Mini Sputter Coater. The surface topography and fiber diameters were subsequently analyzed at various magnifications.

FTIR (Fourier's Transform Infrared Spectroscopy)

The chemical composition and functional groups of the fabricated electrospun fibers were characterized using (FT-IR) spectroscopy (Jasco FT/IR-4700). Spectra were acquired in the

attenuated total reflectance (ATR) mode within the wavenumber range of 4000 to 400 cm^{-1} at a resolution of 4 cm^{-1}. The resulting spectra were systematically analyzed to identify characteristic absorption bands of PCL, collagen, hyaluronic acid, and amniotic membrane components, as well as to evaluate potential intermolecular interactions within the bilayer patches.

Mechanical Analysis

The mechanical properties of the electrospun bilayer patches were evaluated through tensile strength analysis using a universal testing machine (EZ-LX, SHIMADZU Corporation, Japan). Prior to the mechanical characterization, the samples were sectioned into rectangular specimens with standardized dimensions of 10x50 mm. The thickness of each specimen was precisely measured at multiple points using a digital micrometer (Mitutoyo MTI Corp., USA) to ensure accurate cross-sectional area calculations. The results were used to calculate the ultimate tensile strength, elongation at break, and Young's modulus of all samples.

Thermogravimetric Analysis (TGA)

TGA) was performed to evaluate the thermal stability, decomposition profiles, and temperature-dependent mass transitions of the electrospun fiber groups using a Discovery SDT 650 (TA Instruments, USA). For each measurement, approximately 5 mg of the sample was placed in a specialized TGA crucible. To prevent oxidative degradation and ensure an inert environment, the analysis was conducted under a nitrogen atmosphere. The samples were heated from 25°C to 600°C at a constant heating rate of 10°C/min. From the acquired thermograms, both percentage mass loss (TGA) and derivative mass loss (DTG) curves were plotted as a function of temperature to determine the characteristic degradation stages of the polymer-biomaterial composites.

Contact Angle Measurement

The surface wettability and hydrophilicity of the electrospun bilayer patches were evaluated through static (WCA) measurements. The analyses were conducted using an optical goniometer

(OCA 15EC, DataPhysics Instruments GmbH, Germany) at ambient temperature via the sessile drop method. To ensure consistency, the specimens were securely fixed onto a flat stage, and a 3 μL droplet of deionized water was deposited onto the surface using an automated micropipette system. The droplet profile was captured 10 seconds after initial contact using an integrated high-resolution CCD camera. Multiple measurements were recorded from different regions of each sample to determine the average contact angle and evaluate surface homogeneity.

Swelling & Degradation Analysis

The water uptake capacity of the bilayer patches was evaluated through a swelling test. Three specimens from each group (approximately 1.5 mg each) were weighed to obtain their initial dry mass (W_d) using a high-precision analytical balance. The samples were then immersed in Phosphate Buffered Saline (PBS; pH 7.4) and incubated at 37°C to simulate physiological conditions. Swelling rate was calculated via the equation below:

$$Swelling\ Rate\ (\%) = \left(\frac{Ww - Wd}{Ww}\right) * 100$$

Simultaneously, an in vitro degradation study was conducted to determine the mass loss profile over time. The initial dry weights (W_i) were recorded before placing the samples in 1 mL of PBS (pH 7.4) within a shaking incubator at 37°C. At predetermined time intervals, the specimens were retrieved, the PBS was decanted, and the remaining residues were dried in an incubator for 24 hours to ensure complete moisture removal. The final dry weights (W_f) were then measured, and the percentage mass loss was calculated according to the following equation:

$$Mass\ Loss\ (\%) = \left(\frac{Wi - Wf}{Wi}\right) * 100$$

MTT Cell Viability Assay

HDFs (PCS-201-012, ATCC, Maryland) were chosen for *in vitro* cell culture study evaluations. Cells were cultured in DMEM (Capricorn, Germany) supplemented with 10% fetal bovine serum

(FBS; Capricorn, Germany) and 1% penicillin–streptomycin (Gibco, USA) at 37 °C in a humidified incubator with 5% CO_2. Upon reaching 70-80% confluency, cells were passaged using a standard trypsinization method with Trypsin–EDTA (Gibco, USA) and used for subsequent experiments. MTT assay kit ws used to measure the biocompatibility of the fabricated nanofibers. Patches were cut into pieces as same size as the well of 96-well plate and placed inside 96-well plates. After UV sterilization HDFs were seeded onto the nanofibers at a density of 5×10^3 cells/patch. Cells were incubated at 37 °C and 5% CO_2 and cell viability was evaluated on days 1, 3, and 7. At each time point, 100 µL of fresh culture medium was added to each well, followed by the addition of 50 µL of MTT stock solution (E-CK-A341, Elabscience, Wuhan, China). Plates were incubated at 37 °C for 2.5 h, and the absorbance values were recorded at 570 nm using a microplate reader.

Scratch Assay

An *in vitro* scratch assay was performed to evaluate the effects of the nanofibrous patches on the wound-healing and migratory behavior of HDFs. Cells were cultured in DMEM supplemented with 10% FBS and 10,000 units/mL penicillin–streptomycin, and subsequently seeded into well plates at a density of $5x10^4$ cells/well. The cultures were maintained at 37°C in a humidified atmosphere containing 5% CO_2 until 90–100% confluency was achieved.

To simulate a wound, a linear scratch was made in each confluent monolayer using a sterile 200 µL pipette tip. Cellular debris was removed by rinsing the wells twice with sterile PBS. Nanofiber eluates were prepared by incubating the various fiber groups in culture medium at 37°C for 72 hours. The resulting eluates, containing the bioactive factors released from the nanofibers, were subsequently applied to the scratched monolayers.[28] Cells treated with standard culture medium served as the control group. This indirect contact model was utilized to specifically evaluate the influence of soluble components released from the bilayer patches on fibroblast migration without the interference of direct cell-scaffold interactions.

4. Conclusion

In this study, bilayer nanofibrous patches were successfully fabricated by integrating varying concentrations (3%, 5%, 7%, and 10% w/v) of human (AM) into a PCL-based matrix via

electrospinning. The results demonstrated that AM concentration is a decisive factor in determining the morphological, mechanical, and biological properties of the scaffolds. While increasing the AM content led to a gradual decrease in tensile strength due to the disruption of the PCL chain continuity, a critical structural threshold was identified at the 5% concentration in terms of material characterization. This specific group exhibited the finest fiber diameters, leading to a high specific surface area that significantly enhanced the swelling capacity and ductility of the material. The 7% AM group emerged as the optimum formulation for both cell viability and wound-gap repopulation. This finding can be attributed to the balanced interplay between fiber diameter and the accessibility of bioactive components; at the 10% concentration, higher viscosity resulted in larger fibers that potentially sequestered biocomponents within the polymer matrix, making them less accessible for cellular interaction. Overall, these findings suggest that the 7% w/v AM-loaded bilayer nanofibers provide a superior biomimetic microenvironment, positioning them as a highly promising potential biomaterial for advanced wound care and the treatment of ocular surface diseases and many more.

Data Availability

The datasets generated and analysed during the current study are available from the corresponding author on reasonable request

REFERENCES

1. Walkden, A. Amniotic Membrane Transplantation in Ophthalmology: An Updated Perspective . *Clinical Ophthalmology* **14**, 2057–2072 (2020).

2. Hong, M., Tong, L., Mehta, J. S. & Ong, H. S. Impact of Exposomes on Ocular Surface Diseases. *Int. J. Mol. Sci.* **24**, (2023).

3. Ornaghi, H. L., Monticeli, F. M. & Agnol, L. D. A Review on Polymers for Biomedical Applications on Hard and Soft Tissues and Prosthetic Limbs. *Polymers (Basel).* **15**, 4034 (2023).

4. Zhang, H. *et al.* Developing natural polymers for skin wound healing. *Bioact. Mater.* **33**, 355 (2023).

5. Xu, R. *et al.* Recent Advances in Biodegradable and Biocompatible Synthetic Polymers Used in Skin Wound Healing. *Materials* **16**, 5459 (2023).

6. Fénelon, M. *et al.* Applications of Human Amniotic Membrane for Tissue Engineering. *Membranes 2021, Vol. 11, Page 387* **11**, 387 (2021).

7. Mamede, A. C. & Botelhoeditors, M. F. Amniotic membrane: Origin, characterization and medical applications. *Amniotic Membrane: Origin Characterization and Medical Applications* 1–254 (2015) doi:10.1007/978-94-017-9975-1/SAVE-RESEARCH.

8. Dua, H. S., Gomes, J. A. P., King, A. J. & Maharajan, V. S. The amniotic membrane in ophthalmology. *Surv. Ophthalmol.* **49**, 51–77 (2004).

9. Posarelli, M. *et al.* Ocular-Surface Regeneration Therapies for Eye Disorders: The State of the Art. *BioTech 2023, Vol. 12, Page 48* **12**, 48 (2023).

10. Dong, R. *et al.* Electrospun polycaprolactone (PCL)-amnion nanofibrous membrane prevents adhesions and promotes nerve repair in a rat model of sciatic nerve compression. *PLoS One* **15**, 1–16 (2020).

11. Stepanyan, R. *et al.* Nanofiber diameter in electrospinning of polymer solutions: Model and experiment. *Polymer (Guildf).* **97**, 428–439 (2016).

12. Ahmadi Bonakdar, M. & Rodrigue, D. Electrospinning: Processes, Structures, and Materials. *Macromol 2024, Vol. 4, Pages 58-103* **4**, 58–103 (2024).

13. Kristoffersen, K. A. *et al.* FTIR-based prediction of collagen content in hydrolyzed protein samples. *Spectrochim. Acta A Mol. Biomol. Spectrosc.* **301**, (2023).

14. Anaya Mancipe, J. M., Lopes Dias, M. & Moreira Thiré, R. M. D. S. Type I collagen – poly(vinyl alcohol) electrospun nanofibers: FTIR study of the collagen helical structure preservation. *Polymer-Plastics Technology and Materials* **61**, 846–860 (2022).

15. Le Cerf, B. A. *et al.* Nano-Mechanical Analyses of Native and Cross-Linked Collagen I Matrices Reveal the Mechanical Complexity of Homogenous Samples. *Front. Phys.* **10**, 835038 (2022).

16. Sharpe, J. M., Lee, H., Hall, A. R., Bonin, K. & Guthold, M. Mechanical Properties of Electrospun, Blended Fibrinogen: PCL Nanofibers. *Nanomaterials* **10**, 1843 (2020).

17. Hackett, J. M., Dang, T. N. T., Tsai, E. C. & Cao, X. Electrospun biocomposite polycaprolactone/collagen tubes as scaffolds for neural stem cell differentiation. *Materials* **3**, 3714–3728 (2010).

18. Ingraldi, A. L. *et al.* Characterization of Amnion-Derived Membrane for Clinical Wound Applications. *Bioengineering* **11**, 953 (2024).

19. Supriyanto, E. *et al.* Green design of biodegradable packaging films via renewable coffee waste and PVA matrix tuning. https://doi.org/10.1039/d5ra08990e (2026) doi:10.1039/d5ra08990e.

20. Ng, H. M. *et al.* Thermogravimetric Analysis of Polymers. *Encyclopedia of Polymer Science and Technology* 1–29 (2018) doi:10.1002/0471440264.PST667.

21. Govindaraju, D. T., Kao, H. H., Chien, Y. M. & Chen, J. P. Composite Polycaprolactone/Gelatin Nanofiber Membrane Scaffolds for Mesothelial Cell Culture and Delivery in Mesothelium Repair. *International Journal of Molecular Sciences 2024, Vol. 25, Page 9803* **25**, 9803 (2024).

22. Zdraveva, E. *et al.* Electrospun PCL/cefuroxime scaffolds with custom tailored topography. *J. Exp. Nanosci.* **14**, 41–55 (2019).

23. Cho, S. J., Jung, S. M., Kang, M., Shin, H. S. & Youk, J. H. Preparation of hydrophilic PCL nanofiber scaffolds via electrospinning of PCL/PVP-b-PCL block copolymers for enhanced cell biocompatibility. *Polymer (Guildf).* **69**, 95–102 (2015).

24. Martins, A. F. *et al.* Novel poly(ε-caprolactone)/amino-functionalized tannin electrospun membranes as scaffolds for tissue engineering. *J. Colloid Interface Sci.* **525**, 21–30 (2018).

25. Hekmati, A. H., Khenoussi, N., Nouali, H., Patarin, J. & Drean, J. Y. Effect of nanofiber diameter on water absorption properties and pore size of polyamide-6 electrospun nanoweb. *Textile Research Journal* **84**, 2045–2055 (2014).

26. Agarwal, A. *et al.* Natural protein-based electrospun nanofibers for advanced healthcare applications: progress and challenges. *3 Biotech* **12**, (2022).

27. Cândido Lima Verde, T. F. *et al.* Three-Dimensional Printed Hybrid Scaffolds with Layered Polycaprolactone/Nanosized Smectic Clay Nanocomposite and Chitosan/Collagen/Demineralized Bone Powder Hydrogels Targeting Osteochondral Tissue Engineering. *J. Funct. Biomater.* **16**, 441 (2025).

28. Avci, T. *et al.* PLA/BC/lard nanofiber composites as next-generation burn wound dressings. *RSC Adv.* **16**, 14233–14245 (2026).

ACKNOWLEDGEMENT

This study was financially supported by the Turkish Scientific and Technical Research Council (TUBITAK) 1005 Project, Marmara University, Istanbul, Türkiye. The project number is 424S286.

FUNDING

This work was supported and funded by the Turkish Scientific and Technical Research Council (TÜBİTAK) under Grant Number 424S286.

AUTHOR INFORMATIONS

Authors & Affiliations

[1]Department of Metallurgical and Materials Engineering, Faculty of Technology, Marmara University, Istanbul, Turkey

Huseyin Berkay Ozarici, Ayşe Ceren Çalıkoğlu Koyuncu[1], Canan Dogan[1*] & Oguzhan Gunduz[1]

[2]Department Of Ophthalmology, Faculty of Medicine, Marmara University, Istanbul, Turkey

Gamze Ozkan[2]

[3]Acıbadem Mehmet Ali Aydınlar University School of Medicine, Department of Ophthalmology, Istanbul, Türkiye

Semra Akkaya Turhan[3]

[4]Department of Bioengineering, Faculty of Engineering, Marmara University, Istanbul, Turkey

Mohamed Bella Jagitay

[5]Department of Biophysics, Faculty of Medicine, Istanbul Arel University, 34010, Istanbul, Turkey.

Zehra Kanli

CORRESPONDING AUTHORS

Correspondence to Canan Dogan

AUTHOR CONTRIBUTIONS

C.D, O.G., conceived the concept of the study, procured the funding, and were in charge of the overall direction. C.D. and A.C.C.K. designed preliminary study. S.A.T. and G.O. supplied sterilized amniotic membrane from c-section surgery for the experiments. H.B.O. optimized electrospinning production parameters and M.B.J. continued to produce all nanofiber patch groups with optimized parameters. H.B.O. performed all material characterizations and Z.K. performed MTT assay and Scratch model assay with statistical and quantitative analysis. All authors were involved in the preparation and reviewing of the manuscript.

ADDITIONAL INFORMATION

COMPETING INTERESTS

The authors declare that they have no known competing financial interests or personal relationships that could have appeared to influence the work reported in this paper.